Advantages of radial volumetric breath-hold examination (VIBE) with k-space weighted image contrast reconstruction (KWIC) over Cartesian VIBE in liver imaging of volunteers simulating inadequate or no breath-holding ability

Yasunari Fujinaga,[1*] Yoshihiro Kitou,[2] Ayumi Ohya,[1] Yasuo Adachi,[2] Naomichi Tamaru,[2] Aya Shiobara,[2] Hitoshi Ueda,[2] Marcel D Nickel,[3] Katsuya Maruyama,[4] Masumi Kadoya[1]

[1] Department of Radiology, Shinshu University School of Medicine, 3-1-1 Asahi, Matsumoto 390-8621 Japan

Tel: +81-263-37-2650, Fax:+81-263-37-3087

[2] Radiology Division of Shinshu University Hospital, 3-1-1 Asahi, Matsumoto 390-8621 Japan

Tel: +81-263-37-2650, Fax:+81-263-37-3087

[3]Siemens Healthcare GmbH, Erlangen, Germany

[4]Imaging & Therapy Systems Division, Siemens Japan. K. K., Tokyo, Shinagawa, Japan

*The Corresponding author/reprint requests: Yasunari Fujinaga M.D.

Department of Radiology, Shinshu University School of Medicine, 3-1-1 Asahi,

Matsumoto 390-8621, Japan

Tel: +81-263-37-2650, Fax:+81-263-37-3087

e-mail: fujinaga@shinshu-u.ac.jp

Type of manuscript: Original article

Abstract

Objectives To investigate the superiority of radial volumetric breath-hold examination (r-VIBE) with k-space weighted image contrast reconstruction (KWIC) over Cartesian VIBE (c-VIBE) for reducing motion artefact.

Methods We acquired r-VIBE-KWIC and c-VIBE images in 10 healthy volunteers. Each acquisition lasted 24 seconds. The volunteers held their breath for decreasing lengths of time during the acquisitions, from 24 to 0 seconds (protocols A–E). MR images at the level of the right portal vein and confluence of hepatic veins were assessed by two readers using a five-point scale with a higher number indicating a better study.

Results The mean scores for the complete r-VIBE-KWCI series (r-$VIBE_{full}$) and first r-VIBE-KWIC series (r-$VIBE_1$) were not significantly lower than those for c-VIBE in any protocols. The mean scores for c-VIBE were lower than those for r-$VIBE_{full}$ and r-$VIBE_1$ in protocols C and D. The mean score for c-VIBE was lower than that for r-$VIBE_{full}$ in protocol E. The mean score for the eighth r-VIBE-KWIC series (r-$VIBE_8$) was lower than that for c-VIBE only in protocol B.

Conclusion r-VIBE-KWIC minimised artefact relative to c-VIBE at any slice locations. The r-VIBE-KWIC's sub-frame images during the breath-holding period were hardly affected by another failed breath-holding period.

Key points

1. A two-reader study revealed r-VIBE-KWIC's advantages over Cartesian VIBE.

2. The image quality of r-VIBE-KWIC's sub-frame images was maintained during breath-holding.

3. Full-frame r-VIBE-KWIC images minimized motion artefacts caused by breathing.

4. A complete breath-holding over half the acquisition time is recommended for c-VIBE.

5. c-VIBE was susceptible to respiratory motion especially in the subphrenic region.

Keywords: Radial VIBE; k-space weighted image contrast; Dynamic contrast-enhanced MRI; Liver; Motion artifact

Abbreviations

VIBE, volumetric imaging breath-hold examination

KWIC, k-space weighted image contrast reconstruction

DCE-MRI, dynamic contrast-enhanced magnetic resonance imaging

TSM, transient severe motion

Introduction

Dynamic contrast-enhanced magnetic resonance imaging (DCE-MRI) of the liver is usually performed using breath hold gradient echo sequences. Motion artefact may also present a critical problem when the area of interest is subject to respiratory motion. Setting of a short acquisition time can reduce motion artefact, but there is the attendant trade-off between acquisition time and image resolution. The free-breathing radial volumetric imaging breath-hold examination (VIBE) has been reported to provide high quality images without breath-holding; however it necessitates long acquisition times and temporal resolution is sacrificed [1; 2]. Recently, transient severe motion (TSM) in the arterial phase associated with intravenous bolus injection of gadoxetate disodium has been reported [3-6]. It has been attributed to acute transient dyspnoea after intravenous administration of gadoxetate disodium [7]. The implications of this phenomenon are that disordered breathing patterns that may cause motion artefact can occur in patients without underlying respiratory problems. New methods, which maintain a balance between short acquisition time and high image quality, are needed.

Fujinaga et al reported that radial VIBE with k-space weighted image contrast reconstruction (r-VIBE-KWIC) was useful for obtaining high-quality and high-temporal-resolution DCE-MR images without Gibbs ringing artefact in clinical patients [8]. In that study, breath-holding was not examined in each patient. Chandarana et al. reported that the quality of free-breathing radial VIBE images was comparable to that of breath-hold conventional VIBE images [9]. In their setting, breath-holding radial VIBE was impossible because its acquisition time was 56 seconds. In the present study, we aimed to investigate the effect of disordered breathing patterns on VIBE sequences, and whether or not r-VIBE-KWIC has advantages over c-VIBE.

Materials and methods

Subjects

The study protocol was approved by our Institutional Review Board. Written informed consent was obtained from all participating patients before the MRI examinations.

Ten healthy volunteers (nine men and one woman; mean age, 30.8 years; range, 23–46 years), with no history of liver or respiratory disease, were recruited in our institution.

MRI and MR data acquisition

All MR images were obtained with a 3-T MR unit (MAGNETOM Trio, Siemens Healthcare, Erlangen, Germany) using a standard body array coil and a spine matrix coil provided by the manufacturer. MR images of the whole liver were acquired using both prototypical r-VIBE-KWIC and Cartesian VIBE (c-VIBE) sequences, whose scan parameters are shown in Table 1. Scan parameters for each sequence were standardized as far as possible, and were adjusted to be acquired during a breath-hold time of 24 seconds. Parallel imaging was not used in either sequence. In the r-VIBE-KWIC group, MR images yielded eight sub-frame images per one full-frame image using the KWIC view-sharing technique. Eight interleaved subsets of projection views were acquired sequentially to form a full-frame set composed of 208 radial projection views (26 projection views per interleaved subset). In this manner, the volumetric set of contiguous axial images in r-VIBE-KWIC was divided into two subgroups, a dataset of full-frame images (r-$VIBE_{full}$) and a dataset of eight sub-frame images (r-$VIBE_{1–8}$; temporal resolution, 3 seconds). DCE-MRI was not performed because this was a volunteer study and TSM could be simulated without the administration of contrast media.

Breath-holding protocols

MR images were obtained in each subject with five breathing patterns as follows: 1) protocol A: 24-second breath hold, i.e. volunteers held their breath throughout the image acquisition time; 2) protocol B: an 18-second breath-hold followed by 6 seconds of free breathing; 3) protocol C: a 12-second breath hold followed by 12 seconds of free breathing; 4) protocol D: a 6-second breath hold followed by 18 seconds of free breathing; 5) protocol E: free breathing throughout the 24-second image acquisition period.

Imaging analysis

The adequacy of all MR images was qualitatively assessed by two experienced abdominal radiologists (Y. F. and A. O.) independently using a commercial software package (EV Insite; PSP Corporation, Tokyo, Japan). For the assessment, four image datasets, including the full-frame images of r-VIBE-KWIC (r-VIBE$_{full}$), the first sub-frame images of r-VIBE-KWIC (r-VIBE$_1$), the eighth sub-frame images of r-VIBE-KWIC (r-VIBE$_8$), and the c-VIBE images, were used. Because respiratory-induced liver motion is the strongest in the subphrenic region [10], two MR image sections (including the right portal vein [RPV] and the hepatic venous confluence) were selected from each image dataset. The two readers assessed the degree of artefact using a five-point scale (5, no artefact; 4, faint, diagnostic; 3, moderate, diagnostic; 2, intermediate, non-diagnostic; 1, strong, non-diagnostic) that was used in the previous study [8] when assessing the visibility of intrahepatic vessels and the homogeneity of the liver parenchyma (Fig. 1). The mean scores were used for analysis.

Statistical analysis

To compare the values of each breath-holding protocol cluster, we used the Kruskal–Wallis test and Dunn's multiple comparison test. To compare the values in the two slice positions, we used the Wilcoxon matched-pairs signed rank test. All statistical tests were two-tailed, and differences with $P < 0.05$ were regarded as statistically significant. We calculated kappa statistics to evaluate inter-reader agreement. A kappa value of ≤ 0.20 indicated poor agreement; 0.21–0.40, fair agreement; 0.41–0.60, moderate agreement; 0.61–0.80, good agreement; and 0.81–1.00, excellent agreement. The statistical analysis was performed using software (Prism, version 6; GraphPad Software, La Jolla CA, USA and Microsoft Excel 2010; Microsoft, Redmond WA, USA).

Results

The mean scores (range) at the level of the RPV and hepatic venous confluence on r-VIBE$_{full}$, r-VIBE$_{1}$, r-VIBE$_{8}$ and c-VIBE in each protocol are shown in Tables 2 and 3, and distribution of the scores is shown in Figs 1 and 2. Representative images are shown in Figs 3 and 4. The mean scores in r-VIBE$_{full}$ were ≥ 3 (diagnostic) in all protocols, while those in c-VIBE were < 3 in protocols C, D and E (i.e., when the breath-hold time was less than 3/4 of the acquisition time). The mean scores in r-VIBE$_{1}$ were > 3 in all protocols except for protocol E (free breathing throughout the 24-second image acquisition period), and those in r-VIBE$_{8}$ were > 3 only in protocol A (complete breath-hold throughout the acquisition time).

Comparing sequences, in protocol A (complete breath hold throughout the image acquisition time) there was no significant difference in the mean scores among r-VIBE$_{full}$, r-VIBE$_1$, r-VIBE$_8$ and c-VIBE. In protocol B (breath-hold time 3/4 of the acquisition time), the mean score for r-VIBE$_8$ was significantly lower than that for other groups. In protocol C (breath-hold time half of the acquisition time), the mean scores for r-VIBE$_{full}$ and r-VIBE$_1$ were higher than those for r-VIBE$_8$ and c-VIBE. In protocol D (breath-hold time 1/4 of the acquisition time), the mean scores of r-VIBE$_{full}$ and r-VIBE$_1$ were higher than that of c-VIBE. Additionally, the mean score for r-VIBE$_8$ was higher than that for c-VIBE at the level of the hepatic venous confluence. In protocol E (free breathing), the mean score for r-VIBE$_{full}$ was higher than that for r-VIBE$_1$ and c-VIBE at the level of the RPV, and the mean score for c-VIBE was lower than that for r-VIBE$_{full}$ and r-VIBE$_8$ at the level of the hepatic venous confluence.

In r-VIBE$_{full}$ and c-VIBE, the mean scores in protocol A (complete breath hold throughout the image acquisition time) were significantly higher than those in protocols C, D, and E at the two scan levels. In r-VIBE$_1$, the mean score in protocol A was significantly higher than those in protocols D and E at the two scan levels. In r-VIBE$_8$, the mean score in protocol A was significantly higher than those in protocol B, C, D and E at the two scan levels.

Comparing the slice location, in r-VIBE$_{full}$, r-VIBE$_1$, and r-VIBE$_8$, there was no significant difference in the median scores between those at the level of the RPV and the hepatic venous confluence in all protocols. In c-VIBE, there was no significant difference in the median scores between those at the two scan levels in all protocols, with the exception of protocol D ($P < 0.05$).

There were no instances of poor or fair inter-reader agreements, although kappa values between the two readers varied (Table 4).

Discussion

Our results suggest that image quality in r-VIBE$_{full}$ is clinically acceptable even with imperfect or absent breath-holding, but image quality in c-VIBE is clinically unacceptable when the breath hold time was less than 3/4 of the acquisition time (18 seconds in the current study). This indicates an advantage of r-VIBE-KWIC over c-VIBE. We attribute this result to the different trajectory of k-space acquisition. Radial k-space acquisition has an advantage for reducing motion artefact because acquired data repetitively sampled at the central region of the k-space overcome motion artefact [11]. In our study, the mean scores of r-VIBE$_{full}$ were significant higher than those of c-VIBE in protocols C, D and E (breath-hold time was 12, 6 and 0 seconds, respectively) at the two scan levels. Additionally, a significant difference between the median c-VIBE scores at the two scan levels was found in protocol D. This result suggests that c-VIBE acquisitions of the subphrenic region of the liver are more susceptible to respiratory motion artefact compared with r-VIBE$_{full}$ images.

Even though our study included only noncontrast MR images without assessment of detailed structures and lesion detectability, our results suggested that r-VIBE-KWIC was a feasible technique to provide diagnostic sub-frame images with high temporal resolution, as shown by a mean score for r-VIBE$_1$ and r-VIBE$_8$ > 3 with a single breath-hold during the entire acquisition time. However, their mean scores were lower than that for r-VIBE$_{full}$, i.e. there was degradation of the image quality on sub-frame images when the breath hold was less than the length of the 24-second sequence of when the subject breathed normally. We attribute this result to a streak artefact in insufficiently sampled data of the sub-frame images as compared with r-VIBE$_{full}$, which is characteristically seen in radial acquisition sequences; additionally motion correction does not work well as compared with full-frame images [12]. The r-VIBE-KWIC, however, has an advantage in that both full-frame images and sub-frame images can be acquired simultaneously [8]. This characteristic of r-VIBE-KWIC compensates for any shortcomings of sub-frame images if the breath hold is shorter than the acquisition time or if the patient breathes normally.

Although the breath-hold time was longer in protocol D (6 seconds) than in protocol E (0 seconds, i.e., free-breathing), the mean c-VIBE score in protocol D was slightly lower than that in protocol E, especially at the level of the hepatic venous confluence. Although there was no significant difference between the protocols, taking a deep breath after breath holding may be one reason for this. These results could also explain that the occurrence of TSM might be caused by the taking of a deep-breath during the arterial phase of DCE-MRI using Cartesian gradient echo sequences. This phenomenon can occur when breath-holding failed during the arterial phase of

DCE-MRI, independently of the duration of the acquisition time and any kind of contrast agent.

Our study had some limitations. The sample size ($n = 10$) was small, and all volunteers were healthy without liver lesions or chronic liver disease. We did not perform DCE-MRI using contrast agents including gadoxetate disodium, it being unrealistic to perform five injections for our study design, especially injections associated with respiratory discomfort. In addition, assessment of lesion detectability and lesion characteristics was not possible in this study because only normal volunteers were included. We believe that the effects of motion artefact could be assessed using non-contrast MR images and standardized parameters in each sequence provided accurate and detailed results.

In conclusion, r-VIBE-KWIC minimised motion artefact compared with c-VIBE, when breath holding was deliberately made suboptimal. The basic quality of the sub-frame images of r-VIBE-KWIC was preserved throughout the breath-holding component of the acquisition time owing to their high-temporal resolution.

Acknowledgements The scientific guarantor of this publication is Prof. Masumi Kadoya. The authors of this manuscript declare the relationships with the following companies: Dr. Marcel Diminik Nickel is an employee of Siemens Healthcare, and Mr. Katsuya Maruyama is an employee of Siemens Japan K. K. The authors thank these companies for allowing the use of the prototypical r-VIBE-KWIC for our study.

The authors state that this work was supported by a "Grant-in-Aid for Scientific Research" (C) (15K09917) from the Ministry of Education, Culture, Sports, Science and Technology of Japan. No complex statistical methods were necessary for this paper. Institutional review board approval was obtained. Written informed consent was obtained from all subjects (volunteers) in this study. No animal subjects are included in this study. No study subjects or cohorts have been previously reported. Methodology: prospective, diagnostic study, performed at one institution.

References

1 Reiner CS, Neville AM, Nazeer HK, et al. (2013) Contrast-enhanced free-breathing 3D T1-weighted gradient-echo sequence for hepatobiliary MRI in

patients with breath-holding difficulties. Eur Radiol, 23(11):3087-3093. doi: 10.1007/s00330-013-2910-2

2 Chandarana H, Block KT, Winfeld MJ, et al. (2014) Free-breathing contrast-enhanced T1-weighted gradient-echo imaging with radial k-space sampling for paediatric abdominopelvic MRI. Eur Radiol, 24(2):320-326. doi: 10.1007/s00330-013-3026-4

3 Azevedo RM, de Campos RO, Ramalho M, Heredia V, Dale BM, Semelka RC (2011) Free-breathing 3D T1-weighted gradient-echo sequence with radial data sampling in abdominal MRI: preliminary observations. AJR Am J Roentgenol, 197(3):650-657. doi: 10.2214/AJR.10.5881

4 Bamrungchart S, Tantaway EM, Midia EC, et al. (2013) Free breathing three-dimensional gradient echo-sequence with radial data sampling (radial 3D-GRE) examination of the pancreas: Comparison with standard 3D-GRE volumetric interpolated breathhold examination (VIBE). J Magn Reson Imaging. doi: 10.1002/jmri.24064

5 Pietryga JA, Burke LM, Marin D, Jaffe TA, Bashir MR (2014) Respiratory

motion artifact affecting hepatic arterial phase imaging with gadoxetate disodium: examination recovery with a multiple arterial phase acquisition. Radiology, 271(2):426-434. doi: 10.1148/radiol.13131988

6 Davenport MS, Bashir MR, Pietryga JA, Weber JT, Khalatbari S, Hussain HK (2014) Dose-toxicity relationship of gadoxetate disodium and transient severe respiratory motion artifact. AJR Am J Roentgenol, 203(4):796-802. doi: 10.2214/AJR.13.11587

7 Davenport MS, Viglianti BL, Al-Hawary MM, et al. (2013) Comparison of acute transient dyspnea after intravenous administration of gadoxetate disodium and gadobenate dimeglumine: effect on arterial phase image quality. Radiology, 266(2):452-461. doi: 10.1148/radiol.12120826

8 Fujinaga Y, Ohya A, Tokoro H, et al. (2014) Radial volumetric imaging breath-hold examination (VIBE) with k-space weighted image contrast (KWIC) for dynamic gadoxetic acid (Gd-EOB-DTPA)-enhanced MRI of the liver: advantages over Cartesian VIBE in the arterial phase. Eur Radiol, 24(6):1290-1299. doi: 10.1007/s00330-014-3122-0

9 Chandarana H, Block TK, Rosenkrantz AB, et al. (2011) Free-breathing radial 3D fat-suppressed T1-weighted gradient echo sequence: a viable alternative for contrast-enhanced liver imaging in patients unable to suspend respiration. Invest Radiol, 46(10):648-653. doi: 10.1097/RLI.0b013e31821eea45

10 Sutherland J, Pantarotto J, Nair V, Cook G, Plourde M, Vandervoort E (2015) WE-AB-303-05: Breathing Motion of Liver Segments From Fiducial Tracking During Robotic Radiosurgery and Comparison with 4D-CT-Derived Fiducial Motion. Medical physics, 42(6):3656. doi: 10.1118/1.4925870

11 Glover GH, Noll DC (1993) Consistent projection reconstruction (CPR) techniques for MRI. Magn Reson Med, 29(3):345-351.

12 Song HK, Dougherty L (2004) Dynamic MRI with projection reconstruction and KWIC processing for simultaneous high spatial and temporal resolution. Magn Reson Med, 52(4):815-824. doi: 10.1002/mrm.20237

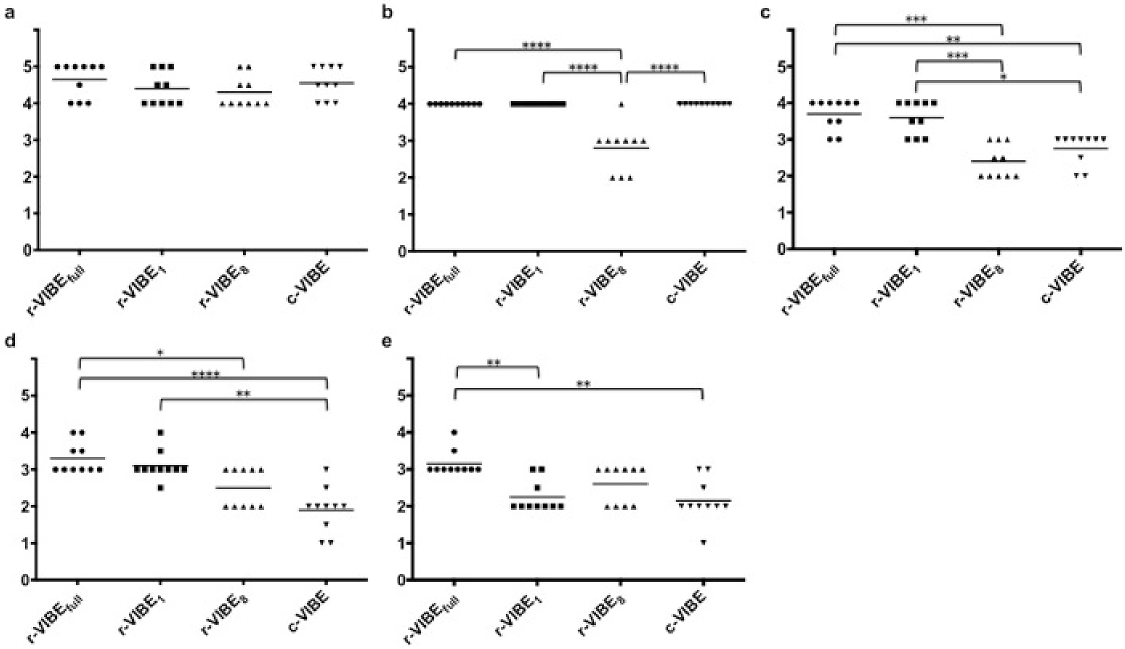

Fig. 1 Distribution of scores at the level of the right portal vein. (a)–(e) show the results in protocols A–E, respectively. *, $P < 0.05$; **, $P < 0.01$; ***, $P < 0.001$; ****, $P < 0.0001$; long bar, mean

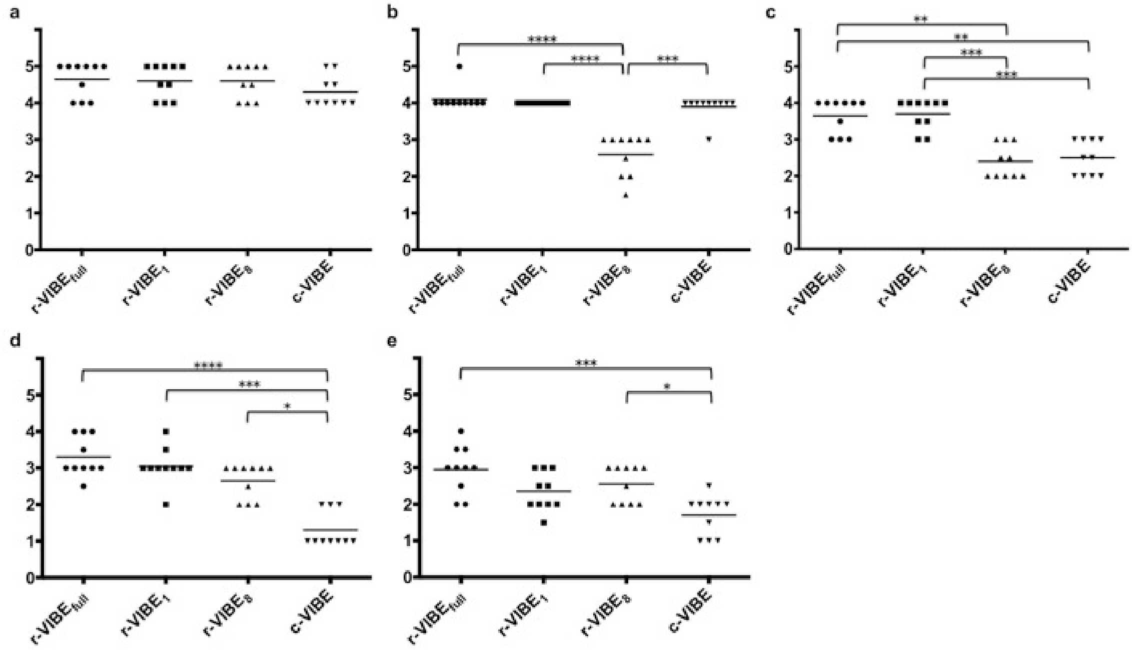

Fig. 2 Distribution of scores at the level of the confluence of the hepatic veins. (a)–(e) show the results in protocols A–E, respectively. *, $P < 0.05$; **, $P < 0.01$; ***, $P < 0.001$; ****, $P < 0.0001$; long bar, mean

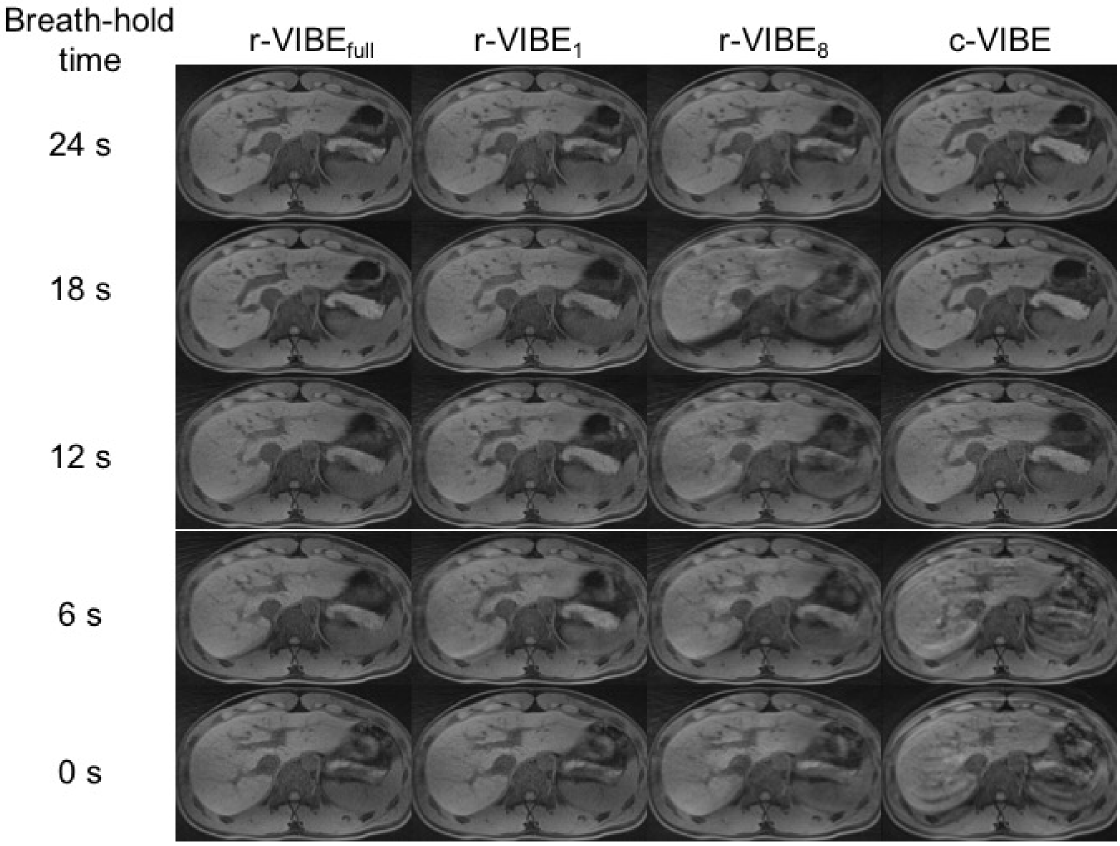

Fig. 3 Representative MR images at the level of the right portal vein. Column: types of sequences; Row: length of breath hold; r-VIBE$_{full}$: full-frame image of radial volumetric breath-hold examination with k-space weighted image contrast reconstruction (r-VIBE-KWIC); r-VIBE$_1$: first sub-frame image of r-VIBE-KWIC; r-VIBE$_8$: eighth sub-frame image of r-VIBE-KWIC; c-VIBE: Cartesian VIBE

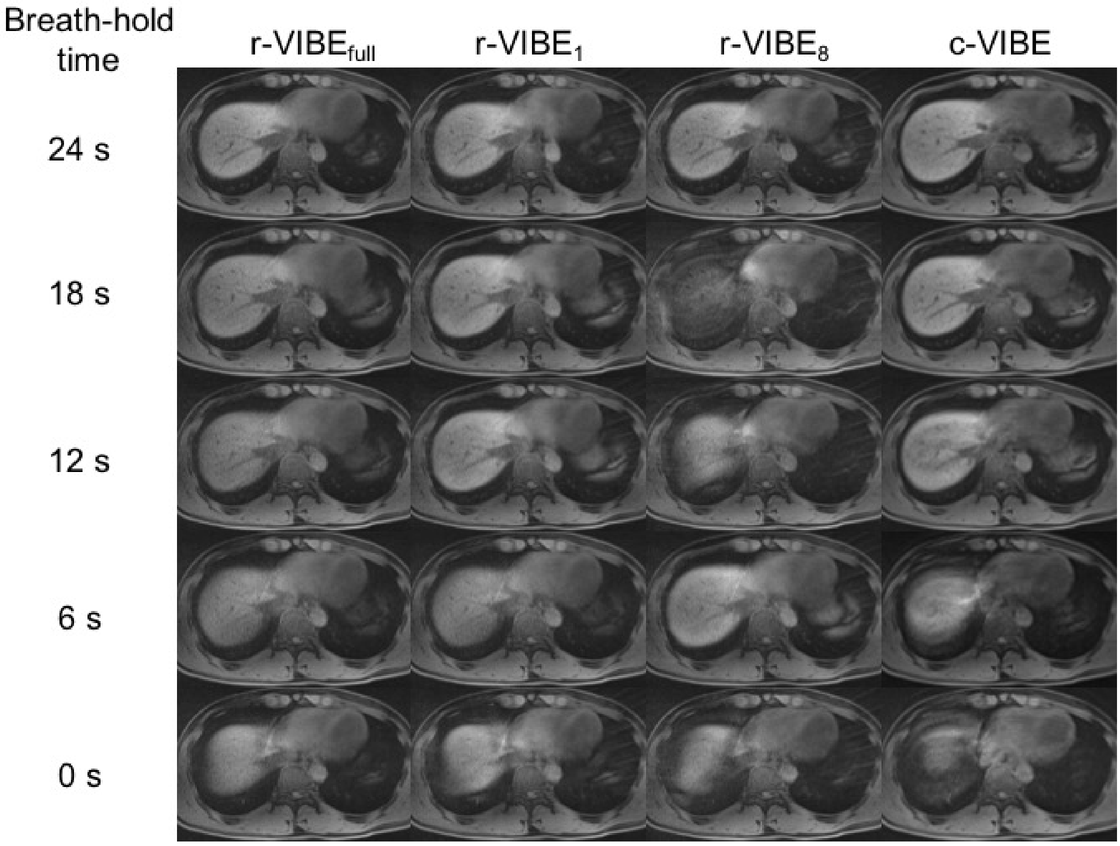

Fig. 4 Representative MR images at the level of the confluence of the hepatic veins. Column: types of sequences; Row: length of breath hold; r-VIBE$_{full}$: full-frame image of radial volumetric breath-hold examination with k-space weighted image contrast reconstruction (r-VIBE-KWIC); r-VIBE$_1$: first sub-frame image of r-VIBE-KWIC; r-VIBE$_8$: eighth sub-frame image of r-VIBE-KWIC; c-VIBE: Cartesian VIBE

Table 1 Scan parameters of the two sequences

	r-VIBE-KWIC[a]	c-VIBE[b]
Repetition time (ms)	2.58	2.58
Echo time (ms)	1.17	1.17
Flip angle (degree)	13	13
Matrix size	192 × 192	192 × 192
Section thickness (mm)	4	4
Field of view (mm)	300 × 300	300 × 300
Acquisition time (s)	24	24
Band width (Hz/pixel)	1530	1530
Parallel imaging	No	No

[a]r-VIBE-KWIC: radial volumetric imaging breath-hold examination with k-space weighted image contrast; [b]c-VIBE: Cartesian VIBE

Table 2 Mean scores (range) at the level of the right portal vein

Protocol (breath-hold time)	r-$VIBE_{full}$[a]	r-$VIBE_1$[b]	r-$VIBE_8$[c]	c-VIBE[d]
A (24 s)	4.7 (4–5)	4.4 (4–5)	4.3 (4–5)	4.6 (4–5)
B (18 s)	4.0 (4)	4.0 (4)	2.8 (2–4)	4.0 (4)
C (12 s)	3.7 (3–4)	3.6 (3–4)	2.4 (2–3)	2.8 (2–3)
D (6 s)	3.3 (3–4)	3.1 (2.5–4)	2.5 (2–3)	1.9 (1–3)
E (0 s)	3.2 (3–4)	2.3 (2–3)	2.6 (2–3)	2.2 (1–3)

[a]r-$VIBE_{full}$: full-frame images of radial volumetric imaging breath-hold examination with k-space weighted image contrast (r-VIBE-KWIC); [b]r-$VIBE_1$: first sub-frame images of r-VIBE-KWIC; [c]r-$VIBE_8$: eighth sub-frame images of r-VIBE-KWIC; [d]c-VIBE: Cartesian VIBE

Table 3 Mean scores (range) at the level of the confluence of the hepatic veins

Protocol (breath-hold time)	r-VIBE$_{full}$[a]	r-VIBE$_1$[b]	r-VIBE$_8$[c]	c-VIBE[d]
A (24 s)	4.7 (4–5)	4.6 (4–5)	4.6 (4–5)	4.3 (4–5)
B (18 s)	4.1 (4–5)	4.0 (4)	2.6 (1.5–3)	3.9 (3–4)
C (12 s)	3.7 (3–4)	3.7 (3–4)	2.4 (2–3)	2.5 (2–3)
D (6 s)	3.3 (2.5–4)	3.1 (2–4)	2.7 (2–3)	1.3 (1–3)
E (0 s)	3.0 (2–4)	2.4 (1.5–3)	2.6 (2–3)	1.7 (1–2.5)

[a]r-VIBE$_{full}$: full-frame images of radial volumetric imaging breath-hold examination with k-space weighted image contrast (r-VIBE-KWIC); [b]r-VIBE$_1$: first sub-frame images of r-VIBE-KWIC; [c]r-VIBE$_8$: eighth sub-frame images of r-VIBE-KWIC; [d]c-VIBE: Cartesian VIBE

Table 4 Kappa values

Protocol (breath-hold time)	$r\text{-}VIBE_{full}$[a]		$r\text{-}VIBE_1$[b]		$r\text{-}VIBE_8$[c]		c-VIBE[d]	
	RPV[e]	HVC[f]	RPV	HVC	RPV	HVC	RPV	HVC
A (24 s)	0.7826	0.7826	0.6000	0.6000	0.5455	0.6000	0.4444	0.5238
B (18 s)	AS[g]	1.0000	AS	AS	1.0000	0.5918	AS	1.0000
C (12 s)	0.5238	0.7826	0.6000	0.5455	0.5833	0.5833	0.7368	0.6154
D (6 s)	0.5238	0.6226	0.4118	0.7561	1.0000	0.7826	0.6491	1.0000
E (0 s)	0.6154	0.5328	0.7368	0.4545	1.0000	0.8000	0.8039	0.6154

[a]$r\text{-}VIBE_{full}$: full-frame images of radial volumetric imaging breath-hold examination with k-space weighted image contrast (r-VIBE-KWIC); [b]$r\text{-}VIBE_1$: first sub-frame images of r-VIBE-KWIC; [c]$r\text{-}VIBE_8$: eighth sub-frame images of r-VIBE-KWIC; [d]c-VIBE: Cartesian VIBE; [e]RPV: at the level of the right portal vein; [f]HVC: at the level of the hepatic venous confluence; [g]AS: all of the scores were the same